BUTTERWORTH HEINEMANN

Polymer Vol. 36 No. 10, pp. 1947–1955, 1995

0032-3861/95/$10.00+0.00

Morphology and crystal structure of an *a* axis oriented, highly crystalline poly(ethylene terephthalate)

Yukishige Kitano*
Toray Research Center Inc., 3–7 Sonoyama 3-Chome, Otsu, Shiga 520, Japan

and Yukio Kinoshita†
Shiga Prefectural Junior College, Hikone, Shiga 522, Japan

and Tamaichi Ashida
School of Engineering, Nagoya University, Chikusa-ku, Nagoya 464-01, Japan
(Received 26 April 1994; revised 27 September 1994)

The morphological structure of an extremely highly crystalline poly(ethylene terephthalate) (PET) which was obtained by very long term annealing after direct esterification was characterized by small angle and wide angle X-ray diffraction, infra-red spectroscopy, and density and fusion measurements. The specimen has a high melting point of 302.5°C, an observed density of 1.468 g cm^{-3} and a calculated density of 1.501 g cm^{-3}. From these results, together with small angle X-ray scattering data and the dependence of the fusion curves on the heating rate, this highly crystalline material is proposed to consist of molecules which are either fully extended or which contain only a few folds. Moreover, the specimen has a good double orientation: the crystallites not only have their *a* axes parallel, but also have their (001) planes approximately parallel to the main plane of the specimen. The structure determined from the X-ray diffraction intensity data is basically consistent with that obtained by Daubeny *et al.*

(Keywords: poly(ethylene terephthalate); morphology; crystal structure)

INTRODUCTION

The mechanical properties of polymers depend on their morphological structures. The structures of polymer are so complicated that they have been the subject of much interest. It is quite obvious that polymeric materials may differ fundamentally in many important aspects according to the manner in which the polymer was prepared, and it is well known that by varying the crystallization and processing conditions it is possible to obtain technologically significant variations in structure and mechanical properties. Many studies have therefore been carried out to establish relationships between the properties and morphological characteristics of polymers[1–5].

Poly(ethylene terephthalate) (PET) is one of the most commercially important polymers. There have thus been extensive investigations concerning the crystallinity and orientation of PET over a range of thermal, stress and deformation conditions in order to achieve a qualitative and quantitative understanding of the effects of structure on the properties of the polymer. Melting points and densities of crystalline regions are quite significant in discussing the structures and properties of high polymers. To date, crystalline PET has been widely accepted as having a melting point of 260°C and a density of 1.455 g cm^{-3}. However, we have prepared an extremely highly crystalline PET sample having a high melting point of over 300°C and an observed density of 1.468 g cm^{-3}. It is the purpose of this paper to describe the results of the morphological and crystallographic investigation of this new and extremely high crystalline PET, and we will consider various structural models during the discussion of our results. Preliminary reports of this work have been made previously[6,7].

EXPERIMENTAL

Preparation of the samples

The materials were obtained by annealing continuously under vacuum for periods of up to 2 after direct esterification of PET, the temperature being raised gradually to 280°C at a rate of 0.5°C day^{-1}. Increments of only 0.2°C per 4 days were used above 280°C to a final value of 290°C for about 6 months. After the annealing process, the sample tube was cooled from the bath temperature to 230°C at a rate of 2°C day^{-1}, and from 230°C to room temperature at 10°C h^{-1}. The

* To whom correspondence should be addressed
† Present address: Izumi, Minaguchi-cho, Shiga 528, Japan

specimens were then characterized at room temperature by infra-red spectroscopy, X-ray diffraction, and fusion, density and viscosity measurements. For comparison, conventional PET yarn was also studied.

Instrumentation and measurements

Infra-red measurements. Infra-red spectra were collected on a Nihon Bunkou DS-402G infra-red spectrometer from samples in KBr discs. The regions around the bands at 973 cm^{-1} and 898 cm^{-1} were expanded to allow as accurate measurement as possible of the absorptions of these bands. The band at 973 cm^{-1} was assigned to the asymmetric C–O stretching mode, and is associated with the *trans* conformation of the –O–C–C–O– group[8–11] along the PET chain. Its intensity is very sensitive to the order in the polymer[9,11], and therefore this band is extremely useful for the measurement of crystallinity in PET. The band at 898 cm^{-1}, on the other hand, was assigned to the CH_2 rocking (*gauche*) mode, and is claimed to be associated with the amorphous component of the PET chain[9,11,12].

X-Ray measurements. Wide angle X-ray diffraction (WAXD) was measured by a counter diffractometer using graphite-monochromated CuKα radiation detected by a scintillation counter, and X-ray diffraction patterns of small regions were recorded with a Norelco microcamera equipped with a 50 μm collimator.

The unit cell dimensions were determined from a least squares fit of the observed 2θ values of 12 indexed reflections from the (001), (0$\bar{1}$1), (010), (011), (0$\bar{1}$3), (003), (0$\bar{2}$4), (005), (0$\bar{4}$3), ($\bar{1}$10), (100) and (1$\bar{1}$1) plane on the X-ray diffraction photographs taken with a STOE cylindrical camera with a diameter of 114.6 mm, which was calibrated by Al foil and urotropin powder using CuKα radiation. Intensity data for the orientation and crystal structure analysis were obtained using the Weissenberg multifilm method and scaled visually and corrected for Lorentz polarization effects.

Small angle X-ray scattering (SAXS) measurements were also made photographically on a Kiessig pinhole camera with a distance of 400 mm between the specimen and the film.

Fusion measurements. A Perkin–Elmer differential scanning calorimeter model 2C was used for the differential scanning calorimetry (d.s.c.) experiments. The analyses were carried out under nitrogen with specimens of ca. 5 mg. The peak areas of the d.s.c. curves were determined by drawing a baseline as indicated, for example, in *Figure 5*. From the measured heat of fusion ΔH_{exp} an apparent degree of crystallinity W_c (d.s.c.) was determined according to

$$W_c \text{ (d.s.c.)} = \Delta H_{exp}/\Delta H^\circ$$

where ΔH° is the heat of fusion (per mole of repeat units) of an ideal PET crystal. In this work we adopted a value of 6.4 kcal mol^{-1} (=33.5 cal g^{-1}) as given by Wunderlich[13].

Density and other measurements. The density was measured at 25°C in a density gradient column filled with a mixture of n-heptane and tetrachloromethane. The intrinsic viscosity [η] was determined from a solution in *o*-chlorophenol at 25°C as 0.3 dl g^{-1}, corresponding to an average molecular weight $\bar{M}_\eta$ of 8000, which is a little lower than that found for conventional PET.

Inorganic residues in the specimen were estimated by fluorescence X-ray analysis and electron probe X-ray microanalysis (EPMA).

RESULTS AND DISCUSSION

Morphological aspects of the specimen

Figure 1 shows the specimen obtained in this experiment. The specimen was grown as a yellow, tabular, crystalline material thickened by layer growth, and showed clear cleavage between layers. Streaks tilted 35–40° to the layers were also detected using the secondary electron image from the X-ray microanalyser, and along the streaks another cleavage was also observed. *Figure 2* shows the microphotographs of the specimen taken using a microcamera with a 0.05 mm pinhole. The X-ray beam was either parallel to the main plane (*Figure 1a*) or perpendicular to the edge plane (*Figure 1b*) of the specimen. The X-ray diffraction photographs of this specimen suggested that this polymer was almost entirely composed of crystalline regions with almost no amorphous regions, because there was little evidence of amorphous haloes in the X-ray diagrams. Usually, X-ray fibre diagrams of polymers show distinct haloes even for highly crystalline specimens. From *Figure 2* we can also see that the distribution of crystal orientations in each layer varies with the location of the layer. It is clear that certain locations are more regularly

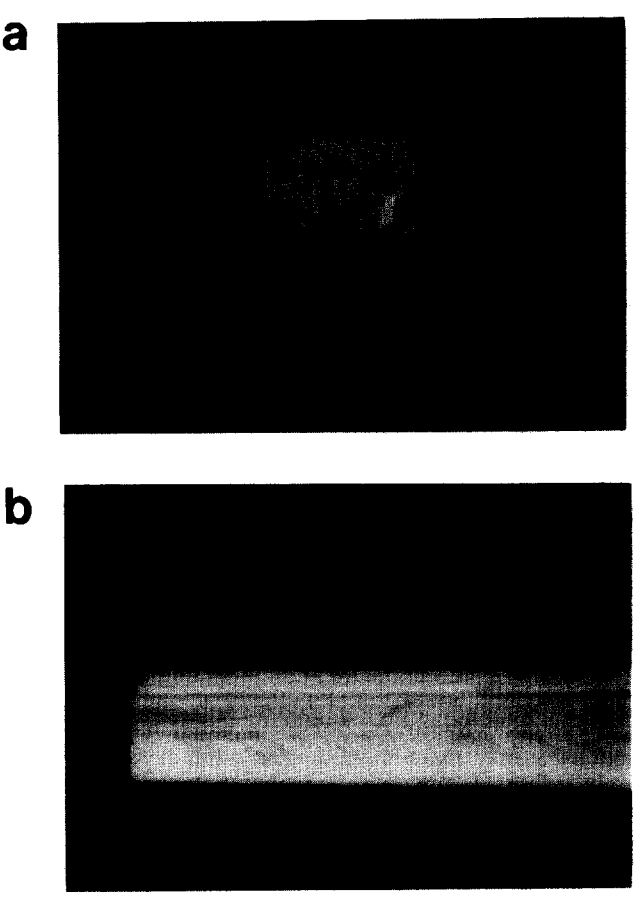

Figure 1 Optical micrographs of the PET specimen: (a) front view (main plane); (b) side view (edge plane). The scale bar corresponds to 3 mm

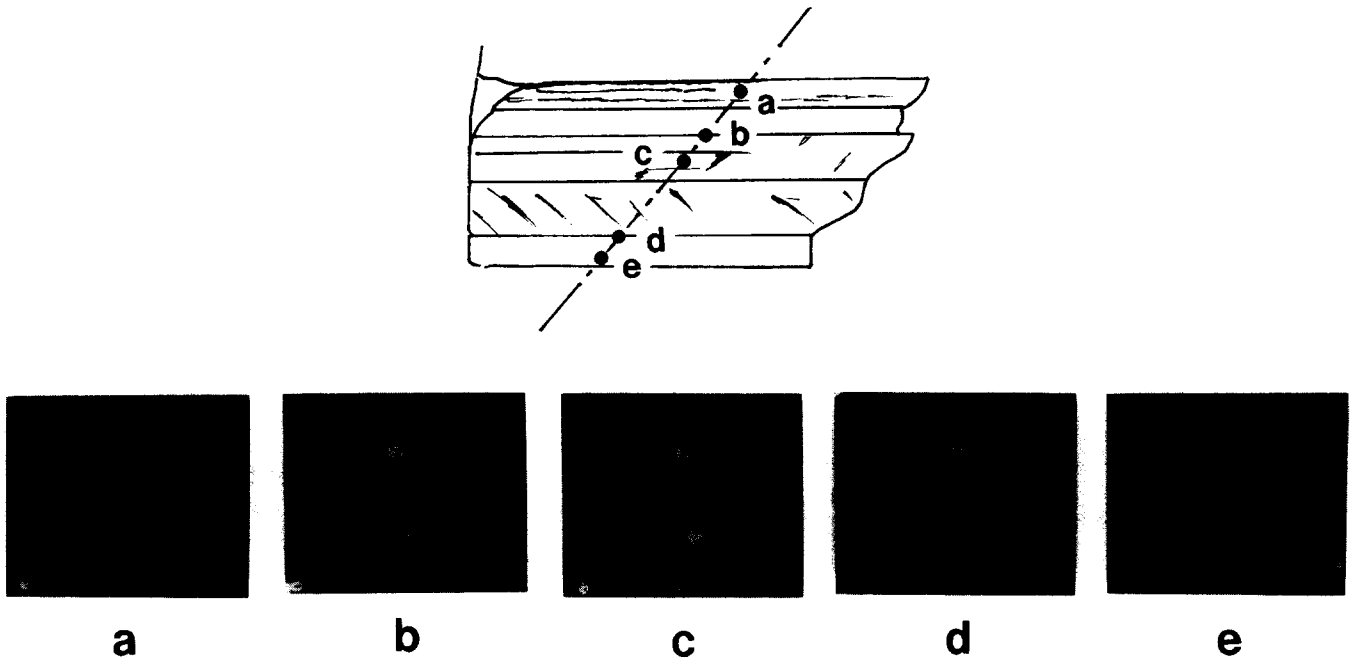

Figure 2 Schematic diagram and X-ray microphotographs of the specimen. The incident beam was parallel to the main plane or perpendicular to the edge plane of the specimen

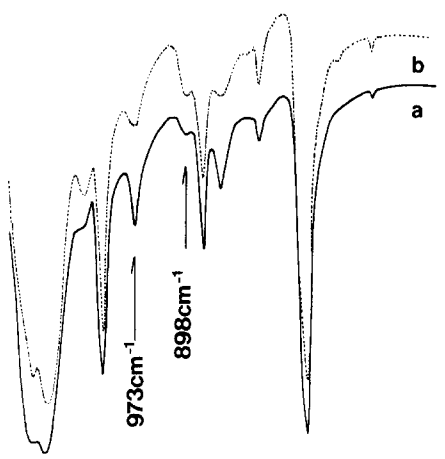

Figure 3 Infra-red spectra of the specimen: (a) original sample; (b) recrystallized sample

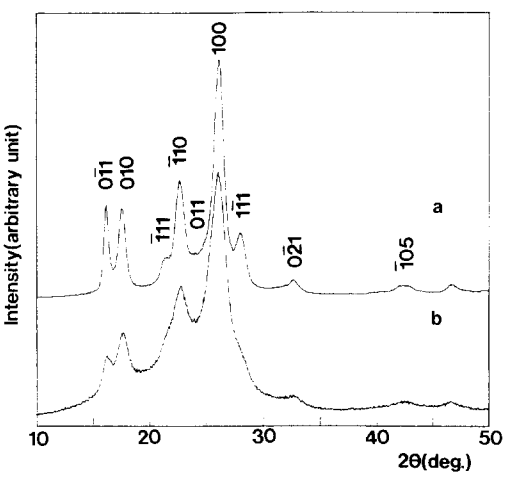

Figure 4 Powder X-ray patterns of (a) our specimen and (b) ordinary PET annealed at 240°C for 30 min

oriented (*Figures 2a–c*) and others more poorly oriented *Figures 2d* and *2e*). For the crystallographic investigation, we selected the most regularly oriented specimen.

Crystallinity

It is interesting and significant that the measured density of the specimen is 1.468 g cm^{-3}, and this value is higher than the well-known crystal density of 1.455 g cm^{-3} calculated by Daubeny *et al.*[14]. If we use this value of crystal density, it is obvious that the degree of crystallinity is more than 100%. Usually, the measured densities of crystalline polymers are lower than the densities of the crystalline regions, owing to the presence of amorphous regions. This means that the crystal density should be higher than this measured density, and it is quite understandable that this crystal density has to be checked. The validity of the crystal density has also been discussed by Mehta *et al.*[15] on the basis of the heat of fusion, and by Fischer and Fakirov[16] and Matyi and Crist[17] on the basis of the SAXS intensity.

The specimen had a residual inorganic content of less than 0.02% as estimated by fluorescence X-ray and EPMA analyses. This amount is within the error range for density measurements (ca. 0.001 g cm^{-3}), so that it will not influence the measured density significantly.

Figure 3 shows the infra-red spectra of the original specimen and the recrystallized specimen. The band at 898 cm^{-1}, assigned to the *gauche* conformation of the –O–C–C–O– group, is weaker than the corresponding band for ordinary PET; the 973 cm^{-1} *trans* band is, on the other hand, stronger than the corresponding band for ordinary PET.

The powder X-ray diffraction pattern of our specimen is shown in *Figure 4* together with the pattern for ordinary

Table 1 Morphological parameters of PET

Sample	Density ($g\,cm^{-3}$)	Heat of fusion ($cal\,g^{-1}$)	Crystallinity			Disorder parameter[c] k	Melting point (°C)
			W_c (dens)[a]	W_c (d.s.c.)[b]	W_c (WAXD)[c]		
Original specimen	1.468	31.9	1.10	0.95	0.84	2.8	302.1
Recrystallized specimen	1.346	13.8	0.10	0.41	0.35	3.1	257.5
Ordinary PET yarn annealed at 240°C for 30 min	1.405	15.1	0.61	0.45	0.60	3.0	260.2

[a] Calculated from density data: $\rho_c = 1.455\,g\,cm^{-3}$, $\rho_a = 1.335\,g\,cm^{-3}$
[b] Calculated from d.s.c. data: $\Delta H^\circ = 33.5\,cal\,g^{-1}$
[c] Obtained by Ruland's method

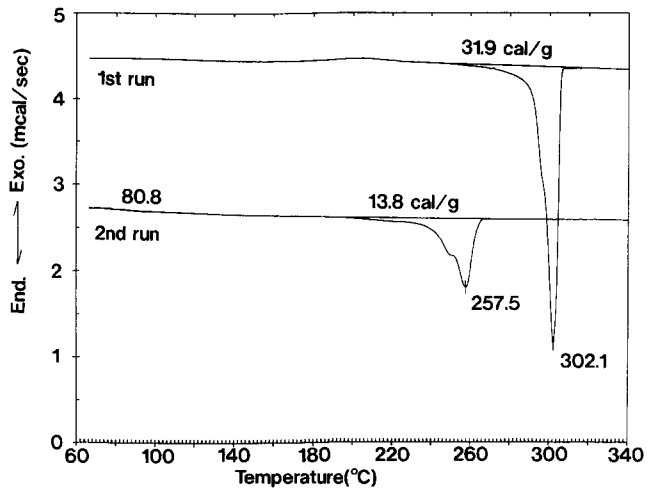

Figure 5 D.s.c. curves of the original specimen (first run) and the recrystallized specimen (second run) measured at 10°C min^{-1}

PET annealed at 240°C for 30 min. The peaks for our specimen are sharp and show a high degree of resolution for the reflections. The crystallinity of our specimen is higher than that of PET annealed at 240°C for 30 min.

In order to estimate the level of crystal perfection, the degree of crystallinity W_c (WAXD) and the disorder parameter k were investigated by Ruland's method[18,19] using a Rigaku-Denki X-ray structure analysis package[20]. The results are shown in *Table 1* together with other morphological parameters of our specimen. A high degree of crystallinity and a low value of k reflect the formation of many perfect crystals in the original specimen.

The d.s.c. curves shown in *Figure 5* indicate that the melting point of our specimen is 302.1°C. After melting and subsequent recrystallization at room temperature, the specimen showed a melting point of 257.5°C in the second run; this is the melting point of ordinary PET. The initial melting point of 302.1°C exceeds most melting points reported so far for PET; for example, the highest observed value is 280°C[21], 284°C has been predicted by Taylor from oligomer melting points[22], and equilibrium melting temperatures (T_m°) of 280°C[15] and 290°C[23] have been calculated according to Hoffman's equation[24]

$$T_m = T_m^\circ(1 - 2\sigma_e/\Delta H^\circ \rho_c l_c)$$

where σ_e is the specific end-surface free energy of the crystals and l_c is their thickness. Our value is approaching the T_m° of 310°C determined by Fakirov *et al.*[25]. Moreover, the observed heat of fusion of 31.9 $cal\,g^{-1}$ leads to a crystallinity W_c (d.s.c.) of 0.95.

Unit cell dimensions

For further characterization of the structure of the original specimen, the unit cell parameters were carefully determined by X-ray diffraction. This new, highly crystalline specimen was a favourable case for crystallographic study, since the specimen showed good double orientation without any treatment. As will be shown later in detail, the crystallites not only have their a axes parallel, but also have their (001) planes approximately parallel to the main plane. In order to determine the cell parameters of the triclinic unit cell of PET, the peak positions of at least six reflections should be established. In this work the unit cell dimensions were determined by least squares fitting from the observed 2θ values of 12 indexed reflections. *Figure 6* shows the positions of the observed ($0kl$) peaks. The calculated peaks based on the cell parameters of Daubeny *et al.*[14] are also shown for comparison. Between the cell parameters there are fairly large differences. The unit cell parameters determined are given in *Table 2* together with all those which have been reported so far. As may be seen from *Table 2*, there are only small differences in the length of the c axis, corresponding to the molecular chain direction of PET, whereas there are rather large differences in the other parameters, corresponding to differences in molecular packing.

As a result, the density calculated from the unit cell dimensions is 1.501 $g\,cm^{-3}$, which is much higher than the values determined by Daubeny *et al.*[14], Tomashpol'skii and Markova[26] and Hall[27], and the same as the value determined by Heuvel and Huisman[28]. Much higher values have been reported by Fakirov *et al.*[29] and Bornschlegl and Bonart[30]. The measured density of the specimen is 1.468 $g\,cm^{-3}$. This value leads to a weight fraction crystallinity of 82%, which is derived from[32]

$$W_c\,(\text{dens}) = \rho_c(\rho - \rho_a)/\rho(\rho_c - \rho_a)$$

where ρ represents the measured density and ρ_c and ρ_a are the density of a 100% crystalline specimen and that of a completely amorphous specimen, respectively.

Crystal perfection

In order to determine the level of crystal perfection it is important to study the dependence of the fusion curves on the heating rate during the d.s.c. measurements[33]. The melting peak temperatures of the original sample and the

Table 2 Unit cell parameters of PET

	Present work	Daubeny *et al.*[14]	Tomashpol'skii and Markova[26]	Hall[27]	Heuvel and Huisman[28]	Fakirov *et al.*[29]	Bornschlegl and Bonart[30]	Fu *et al.*[31]
a (Å)	4.50	4.56	4.52	4.52	4.48	4.48	4.44	4.5087
b (Å)	5.90	5.94	5.98	5.92	5.88	5.85	5.91	5.8818
c (Å)	10.76	10.75	10.77	10.70	10.71	10.75	10.67	10.7873
α (°)	100.3	98.5	101	99.8	100.1	99.5	100.1	100.01
β (°)	118.6	118	118	117.5	117.9	118.4	117.0	118.36
γ (°)	110.7	112	111	111.4	110.7	111.2	111.8	110.56
V (Å^3)	212.5	219.0	216.0	215.5	212.5	210.5	210.6	214.6
d_{calc} (g cm^{-3})	1.501	1.455	1.477	1.479	1.501	1.515	1.515	1.486
d_{obs} (g cm^{-3})	1.468	1.41						

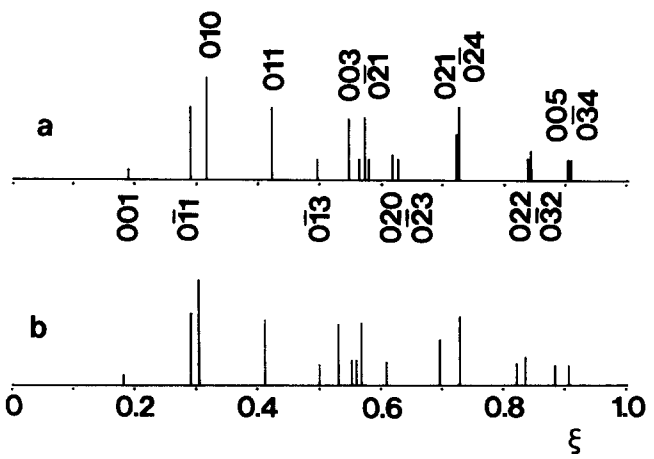

Figure 6 Positions of (a) observed and (b) calculated (0*kl*) peaks. Calculated peaks are based on the data from Daubeny *et al.*[14] and the intensity scale is relative

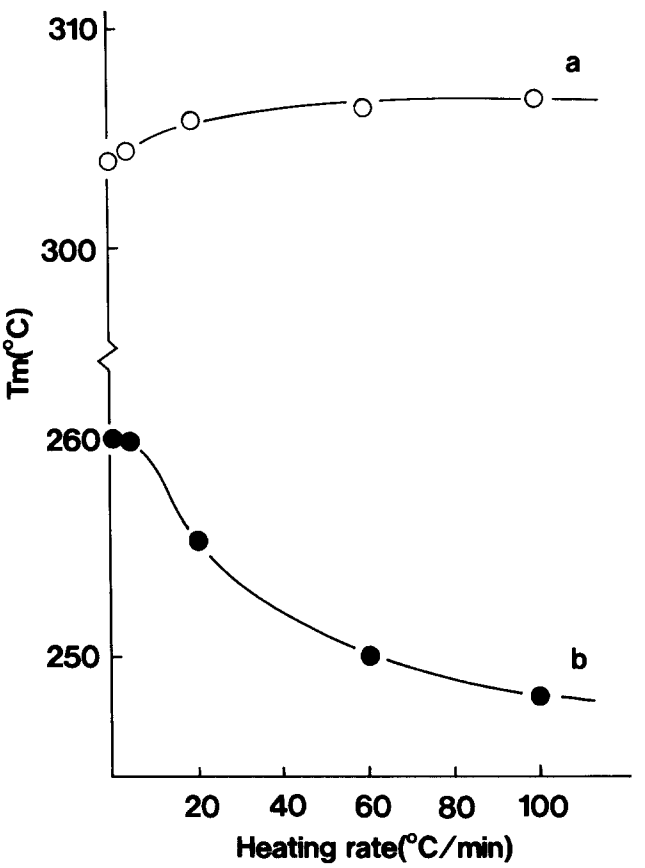

Figure 7 D.s.c. melting peak temperatures as a function of heating rate: (a) original sample; (b) recrystallized sample

recrystallized sample are plotted in *Figure 7* as a function of heating rate. The original sample showed a slight superheating at the faster heating rates. This superheating is caused by the slow melting of polymer crystals which are either fully extended or which contain only a few folds. The recrystallized sample, however, showed a decrease in melting peak temperature with heating rate, which indicates 'continuous melting and recrystallization', i.e. 'reorganization', during heating[34,35].

In addition to the remarkably high density and high melting point, this novel material has a unique property. We attach significance to the data from small angle X-ray scattering experiments. As shown in *Figure 8b*, the recrystallized specimen exhibits a circular, discrete scattering peak at about 100 Å which we can interpret in terms of the periodically spaced blocks of folded chain lamellae in the specimen. The SAXS pattern of the original specimen is distinctive in that no small angle diffraction or scattering can be discerned, indicating either a lack of electron density differences within the resolution of the camera or, as we feel more likely, that the density differences are distributed as small regions throughout the structure. From these SAXS results, together with the high melting point and high crystallinity, we propose that this highly crystalline material consists of molecules which are either fully extended or which contain only a few folds.

Various models have been proposed for the morphological structure of crystalline PET. The models of Statton[36] and Bonart[37] are based on the fringed micelle assumption and have a regular alternation of ordered (crystalline) and disordered (amorphous) regions. Bonart and Hosemann[38] and Fischer and Goddar[39], on the other hand, have proposed, the folded chain structure. The morphological changes proposed for the deformation process of polyethylene by Peterlin and coworkers[40-42] and for annealed nylon 66 fibres by Dismore and Statton[43] are also based on the folding of the molecular chain. In contrast to these models, Keller and Machin[44] have proposed for polyethylene that the nucleation process is associated with the formation of crystals of extended chains from the oriented molecules, and that

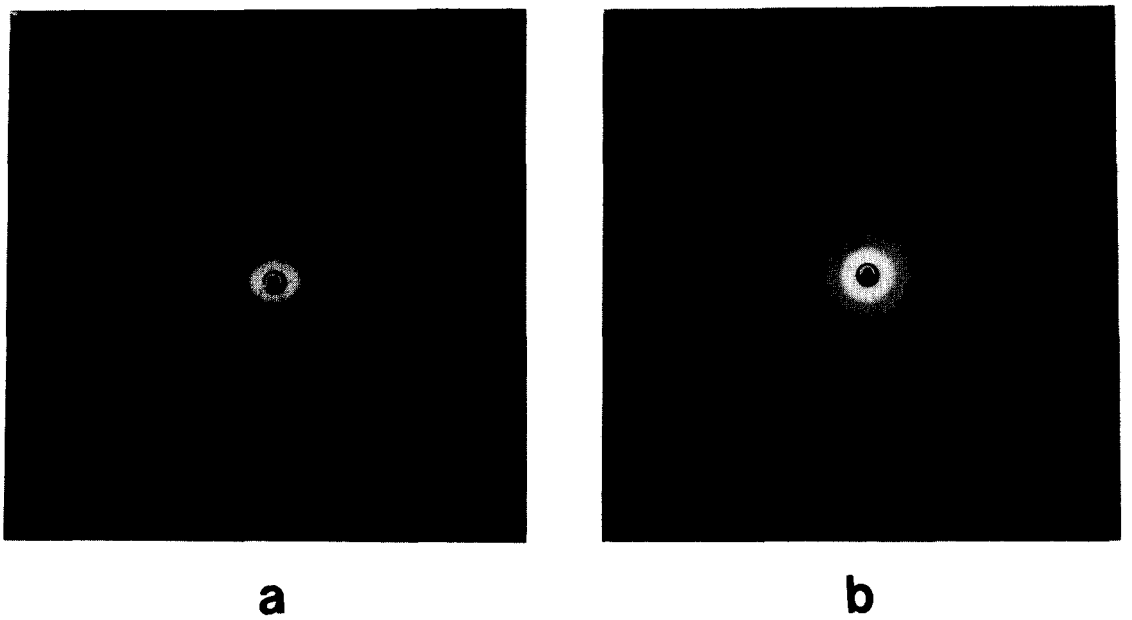

Figure 8 SAXS diagrams of (a) the original specimen and (b) the recrystallized specimen

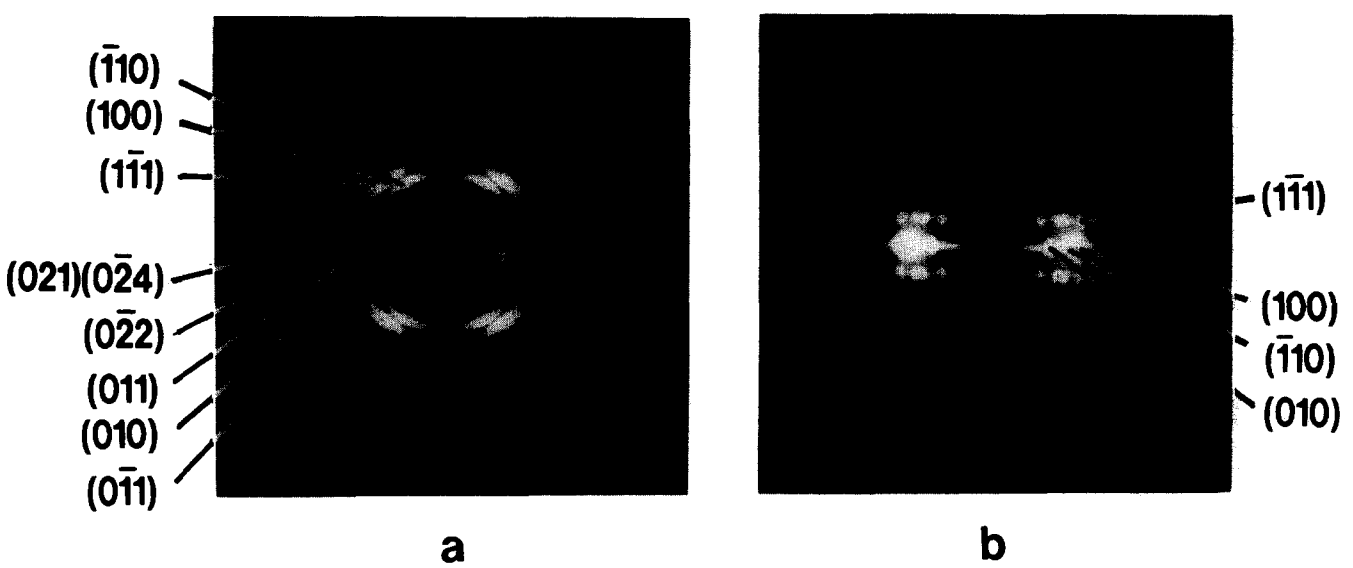

Figure 9 X-ray fibre photographs of (a) our original specimen and (b) ordinary PET yarn annealed at 240°C for 30 min

lamellar crystals grow by chains folding onto these nuclei. We believe that the morphological structure of this highly crystalline PET is similar to that proposed by Clark and coworkers[45,46] for superdrawn acetal and polypropylene, in which the amorphous regions (chain folds) are distributed at random as defects within a continuous crystal matrix of extended chains.

Elucidation of a axis orientation

Figure 9 compare the X-ray diagrams of our specimen and ordinary PET fibre. For comparison, in this experiment the specimen was rotated during the X-ray exposure with the incident X-ray beam perpendicular to the *a* axis. We can see that this highly crystalline PET shows *a* axis orientation, corresponding to a layer of benzene rings making up the short axis of 4.5 Å, while ordinary PET shows *c* axis orientation, corresponding to the fibre direction.

The *a* axis orientation of PET was recognized in the early stages of the fibre-drawing process. The first mention of *a* axis orientation appeared in 1964 by Kuriyama and Shirakashi[47] for slightly stretched fibres having various thermal histories, followed in 1973 by Liska[48] who described the existence of *a* axis orientation for winding speeds in the range 1450–4000 m min^{-1} and observed the transition from *a* axis to *c* axis orientation in the yarn after annealing. The mechanism of the formation of *a* axis orientation has been proposed by Bonart[49] as the folding of molecular chain fibrils. Biangardi and Zachmann[50] also obtained *a* axis orientation by the crystallization of poorly oriented PET film, and explained their results by means of a model twisted lamellar structure. However, as far as we know ours is

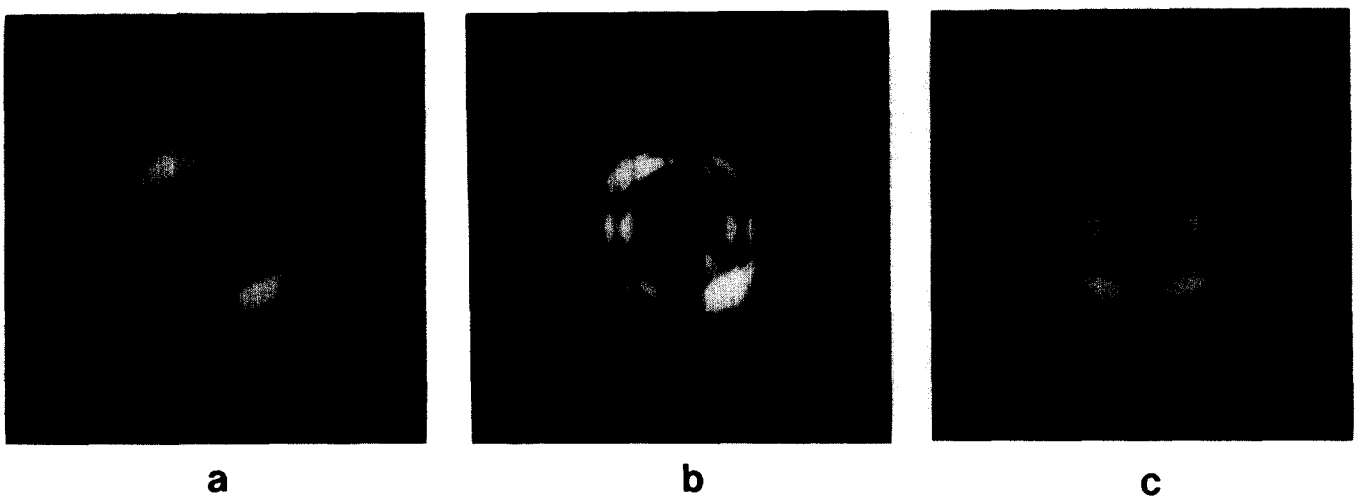

Figure 10 X-ray diagrams of the stationary specimen. The X-ray beam was perpendicular to the *a* axis and (a) parallel, (b) at 45° and (c) perpendicular to the main plane

the first case where the *a* axis orientation has been observed in extremely highly crystalline and fairly well-oriented specimens, although the mechanism of this orientation remains unknown.

Figure 10 shows the X-ray diagrams of the stationary specimen taken perpendicular to the *a* axis. This tabular, crystalline specimen was found to be doubly oriented: the crystallites not only had their *a* axes parallel, but also their (001) planes were approximately parallel to the main plane. In other words, the c^* axes of the crystallites were approximately perpendicular to the main plane of the specimen. Because the specimen was grown naturally, its double orientation was much better than that of a pressed or rolled specimen, in which there is usually some departure from parallelism, especially for the second (planar) orientation. This specimen was a favourable case for crystallographic study since it showed good double orientation without any treatment. *Figure 10a* shows the X-ray diagram of the stationary specimen (not rotated) taken from the edge plane with the incident X-ray beam parallel to the main plane and perpendicular to the *a* axis; a pattern with a centre of symmetry is observed. *Figure 10c* shows the X-ray diagram of the stationary specimen taken from the main plane with the incident X-ray beam perpendicular to the *a* axis; a pattern with mirror symmetry is observed. The pattern in *Figure 10b* is intermediate. These figures are like oscillation photographs of single crystals oscillated over a small angle, this angle corresponding to the dispersion of orientation in the specimen.

It is usual for a triclinic cell for there to be four different possible orientations in the polycrystalline polymer, as shown in *Figure 11*[51]. The results mentioned above, however, indicate that our sample shows only two of these possible orientations (that is, a combination of either the top two or the bottom two orientations in *Figure 11*). This evidence suggests that crystal growth in a particular direction is predominant, i.e. there is a major crystal habit. In a more detailed investigation we took a Weissenberg photograph of the equator line, (0*kl*). *Figure 12* shows the Weissenberg photograph and a schematic diagram for its interpretation in terms of (0*kl*) reflections. From this diagram we can see that the (001) plane is the favoured plane of the twinned crystallites.

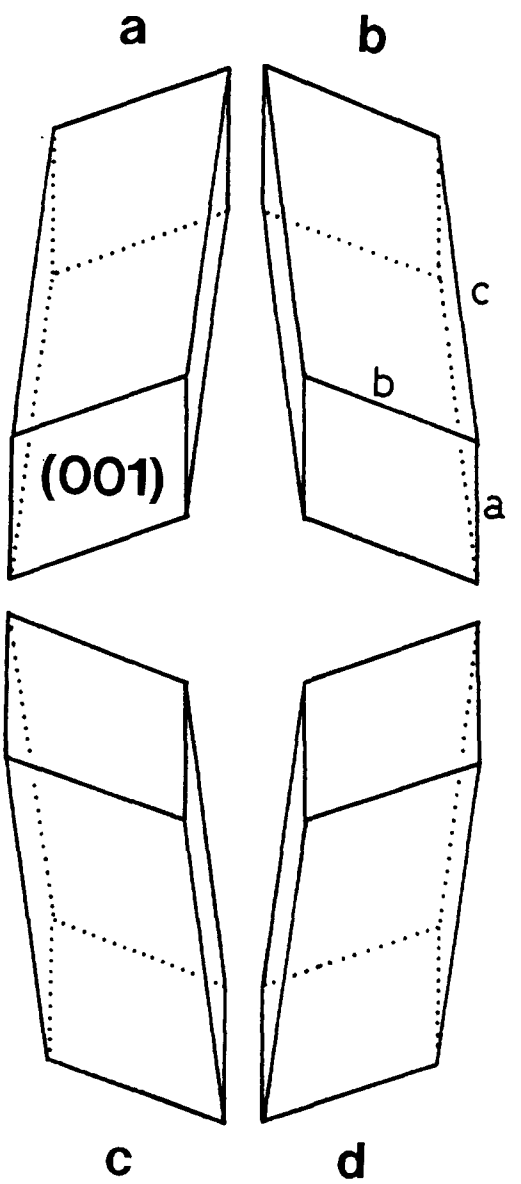

Figure 11 The four possible orientations of the triclinic unit cell

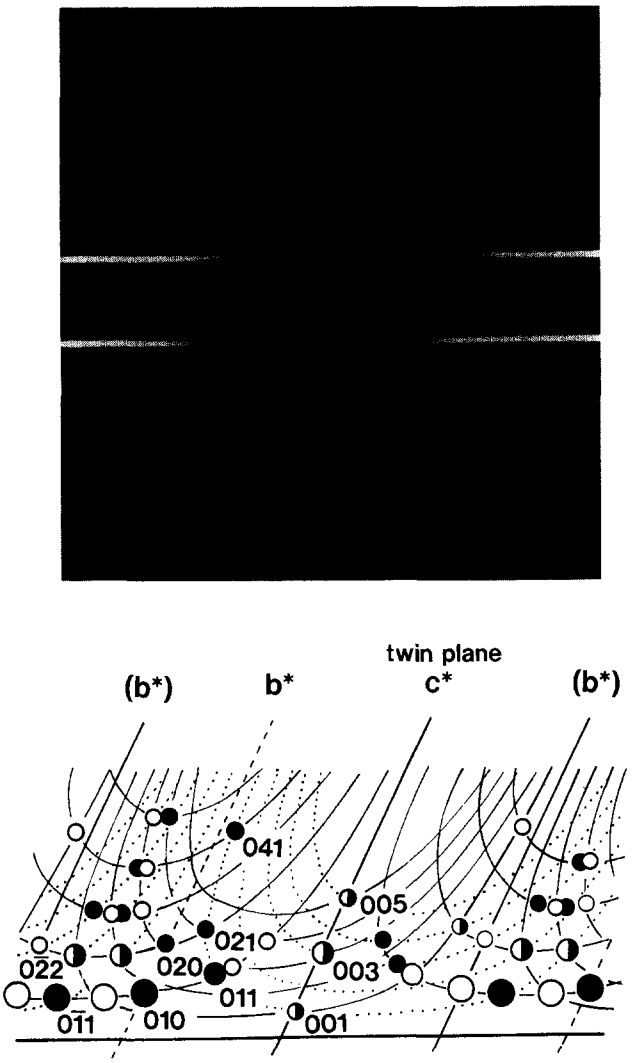

Figure 12 Weissenberg photograph and its interpretation in terms of (0*kl*) reflections

Crystal structure

In order to investigate the crystal structure of this highly crystalline PET, X-ray photographs were taken at an interval of 15° between the two photographs in *Figures 10a* and *10c* and the intensities were visually estimated.

Several cycles of least squares refinements, starting from the atomic coordinates obtained by Daubeny *et al.*[14], were calculated. The *R* factor decreased to 10%. The principal dimensional parameters are shown in *Table 3*, together with other values reported to date. Dimensional parameters for related small molecules are also included in *Table 3* for comparison. These results show that the structure obtained in the present work is basically consistent with that determined by Daubeny *et al.* in 1954, although there are small differences in the atomic dimensional parameters as the unit cell parameters obtained are not the same. It is also interesting that the values determined by Fu *et al.*[31] by the full pattern (two-dimensional Rietveld) fibre refinement method are quite different from other data determined by the traditional integrated intensity refinement methods, especially for the C1′–C1–O1 bond angle and the C2–O1–C1–C1′ conformation angle.

CONCLUSIONS

The extremely highly crystalline PET obtained has several striking features. The melting point of 302.5°C is higher than that of ordinary PET and the observed density of 1.468 g cm^{-3} is also higher than the calculated density of 1.455 g cm^{-3} for the crystalline region. The observed unit cell is smaller than that of ordinary PET. From these results, together with the data from SAXS and the dependence of the fusion curves on the heating rate, this highly crystalline material is proposed to consist of molecules which are either fully extended or which contain only a few folds.

Table 3 Principal dimensional parameters of PET and related compounds

	PET			Ethylene glycol dibenzoate[52]	Ethylene glycol *p*-dichlorobenzoate[53]	PET linear dimer[54]
	Daubeny *et al.*[14]	Fu *et al.*[31]	Present work			
C1–C1′ (Å)	1.471	1.462	1.45	1.499	1.493	1.51
C2–C3 (Å)	1.480	1.484	1.55	1.477	1.482	1.48
C2–O1 (Å)	1.351	1.338	1.33	1.339	1.344	1.337
O1–C1 (Å)	1.446	1.424	1.41	1.442	1.452	1.442
C1′–C1–O1 (°)	104.9	111.7	104	105.2	107.3	104.2
C1–O1–C2 (°)	114.4	117.0	117	115.7	115.8	116.7
O1–C2–C3 (°)	110.1	112.4	113	113.0	112.5	112.8
C2–O1–C1–C1′ (°)	158.7	126.0	167	175.0 −176.1	−175.6	161.9
C3–C2–O1–C1 (°)	−178.2	174.9	−174	−176.0 176.4	−176.0	177.7

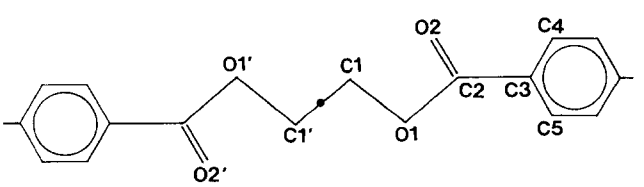

This new crystalline specimen shows good double orientation without any treatment: the crystallites not only have their *a* axes parallel, but they also have their (001) planes approximately parallel to the main plane of the specimen. In our PET specimen, there are only two directions of unit cell orientation and crystal growth in a particular direction is predominant, although usually for a triclinic unit cell there are four different orientations in a doubly oriented specimen. The structure determined from the intensity data is basically consistent with that obtained by Daubeny *et al.*, although there are small differences between the atomic dimensional parameters.

ACKNOWLEDGEMENTS

The authors are grateful to S. Arai of Toray Industries Inc. and H. Iwanaga and T. Hosoi of Toray Research Center Inc. for their technical assistance.

REFERENCES

1 Ward, I. M. 'Mechanical Properties of Solid Polymers', Interscience, New York, 1971
2 Samuels, R. J. *J. Polym. Sci. (A-2)* 1972, **10**, 781
3 Prevorsek, D. C., Kwon, Y. D. and Sharma, R. K. *J. Mater. Sci.* 1977, **12**, 2310
4 Schulz, J. M. and Fakirov, S. (Eds) 'Solid State Behavior of Linear Polyesters and Polyamides', Prentice-Hall, Englewood Cliffs, NJ, 1990
5 Dosiere, M. (Ed.) 'Crystallization of Polymers', Kluwer, Dordrecht, 1992
6 Kitano, Y., Kashiwagi, M., Nukada, K. and Kinoshita, Y. in 'Preprints of the 21st Polymer Symposium', Japan, 1972, p. 537
7 Kinoshita, Y., Nakamura, Y., Kitano, Y. and Ashida, T. *Polym. Prepr.* 1979, **20**, 454
8 Cobbs Jr, W. H. and Burton, R. L. *J. Polym. Sci.* 1953, **10**, 275
9 Miyake, A. *J. Polym. Sci.* 1959, **38**, 479
10 Hannon, M. J. and Koenig, J. L. *J. Polym. Sci. (A-2)* 1969, **7**, 1085
11 Aharoni, S. M., Sharma, R. K., Szobota, J. S. and Vernick, D. A. *J. Appl. Polym. Sci.* 1983, **28**, 2177
12 Miller, R. G. and Willis, H. A. *J. Polym. Sci.* 1956, **19**, 485
13 Wunderlich, B. *Polym. Eng. Sci.* 1978, **18**, 431
14 de P. Daubeny, R., Bunn, C. W. and Brown, C. J. *Proc. R. Soc. London, Ser. A* 1954, **226**, 531
15 Mehta, A., Gaur, U. and Wunderlich, B. *J. Polym. Sci., Polym. Phys. Edn* 1978, **16**, 289
16 Fischer, E. W. and Fakirov, S. *J. Mater. Sci.* 1976, **11**, 1041
17 Matyi, R. J. and Crist Jr, B. *J. Macromol. Sci., Phys. B* 1979, **16**, 15
18 Ruland, W. *Acta Crystallogr.* 1961, **14**, 1180
19 Fontaine, F., Ledent, J., Groeninckx, G. and Reynaers, H. *Polymer* 1982, **23**, 185
20 'RAD-B System Application Software Manual MJ201PZ5', Rigaku-Denki Corporation, Tokyo, 1990
21 Nealy, D. L., Davis, T. G. and Kibler, G. J. *J. Polym. Sci. (A-2)* 1970, **8**, 2141
22 Taylor, G. W. *Polymer* 1962, **3**, 543
23 Groeninckx, G., Reynaers, H., Berghmans, H. and Smets, G. *J. Polym. Sci., Polym. Phys. Edn* 1980, **18**, 1311
24 Lauritzen Jr, J. I. and Hoffman, J. D. *J. Res. Nat. Bur. Stand., Sect. A* 1960, **64**, 73
25 Fakirov, S., Fisher, E. W., Hoffmann, R. and Schmidt, G. F. *Polymer* 1977, **18**, 1121
26 Tomashpol'skii, Y. Y. and Markova, G. S. *Polym. Sci. USSR* 1964, **6**, 316
27 Hall, I. H. (Ed.) 'Structure of Crystalline Polymers', Elsevier, New York, 1984, p. 58
28 Heuvel, H. M. and Huisman, R. *J. Appl. Polym. Sci.* 1978, **22**, 2229
29 Fakirov, S., Fischer, E. W. and Schmidt, G. F. *Makromol. Chem.* 1975, **176**, 2459
30 Bornschlegl, E. and Bonart, R. *Colloid Polym. Sci.* 1980, **258**, 319
31 Fu, Y., Busing, W. R., Jin, Y., Affholter, K. A. and Wunderlich, B. *Macromolecules* 1993, **26**, 2187
32 Alexander, L. E. 'X-ray Diffraction Methods in Polymer Science', Wiley-Interscience, New York, 1969, p. 189
33 Wunderlich, B. 'Macromolecular Physics', Vol. 3, Academic Press, New York, 1980, p. 214
34 Holdsworth, P. J. and Turner-Jones, A. *Polymer* 1971, **12**, 195
35 Miyagi, A. and Wunderlich, B. *J. Polym. Sci. (A-2)* 1972, **10**, 1401
36 Statton, W. O. *J. Polym. Sci.* 1959, **41**, 143
37 Bonart, R. *Kolloid Z. Z. Polym.* 1964, **199**, 136
38 Bonart, R. and Hoseman, R. *Makromol. Chem.* 1960, **39**, 105
39 Fischer, E. W. and Goddar, H. *J. Polym. Sci. (C)* 1969, **16**, 4405
40 Peterlin, A. *Polym. Eng. Sci.* 1977, **17**, 183
41 Peterlin, A. *J. Mater. Sci.* 1971, **6**, 490
42 Ingram, P., Kiho, H. and Peterlin, A. *J. Polym. Sci. (C)* 1967, **16**, 1857
43 Dismore, P. F. and Statton, N. O. *J. Polym. Sci. (B)* 1964, **2**, 1116
44 Keller, A. and Machin, M. J. *J. Macromol. Sci., Phys. B* 1967, **1**, 41
45 Clark, E. S. and Scott, L. S. *Polym. Eng. Sci.* 1974, **14**, 682
46 Taylor, W. N. and Clark, E. S. *Polym. Eng. Sci.* 1978, **18**, 518
47 Kuriyama, J. and Shirakashi, K. *Sen-i Gakkaishi* 1964, **20**, 525
48 Liska, E. *Kolloid Z. Z. Polym.* 1973, **251**, 1028
49 Bonart, R. *Kolloid Z. Z. Polym.* 1969, **231**, 438
50 Biangardi, H. J. and Zachmann, H. G. *Makromol. Chem.* 1976, **117**, 1173
51 Bunn, C. W. 'Chemical Crystallography', 2nd Edn, Oxford University Press, London, 1961, p. 192
52 Perez, S. and Brisse, F. *Acta Crystallogr. B* 1976, **32**, 470
53 Perez, S. and Brisse, F. *Can. J. Chem.* 1975, **53**, 3551
54 Kitano, Y., Ishitani, A. and Inoue, T. *Acta Crystallogr. C* 1991, **47**, 363